https://doi.org/10.1016/j.gete.2021.100264

Calculation of the representative temperature change for the thermomechanical design of energy piles

Huaibo Song

Department of Geotechnical Engineering, Dalian University of Technology, State Key Laboratory of Coastal and Offshore Engineering, Dalian, China

E-mail: songhuaibo@mail.dlut.edu.cn

Huafu Pei*

Department of Geotechnical Engineering, Dalian University of Technology, State Key Laboratory of Coastal and Offshore Engineering, Dalian, China

E-mail: huafupei@dlut.edu.cn

Chao Zhou

Department of Civil and Environmental Engineering, The Hong Kong Polytechnic University, Hung Hom, Kowloon, HKSAR, China

E-mail: c.zhou@polyu.edu.hk

Dujian Zou

Department of Civil and Environmental Engineering, Harbin Institute of Technology, Shen Zhen, China

E-mail: zoudujian@163.com

Chunyi Cui

School of Transportation Equipments and Ocean Engineering, Dalian Maritime University, Dalian, China

E-mail: cuichunyi@dlmu.edu.cn

Corresponding author:

Huafu Pei

Department of Geotechnical Engineering, Dalian University of Technology,

Dalian, 116024, China

E-mail: huafupei@dlut.edu.cn

Abstract

In the geotechnical design of energy piles using various methods such as simplified one-dimension analyses and finite element simulations, the pile temperature change is a crucial input parameter. The current analysis methods usually ignore the non-uniformity of temperature over the pile cross-section and adopt the maximum temperature change as the input parameter. However, this method cannot correctly describe the thermomechanical performance of energy piles and may lead to over-design. This paper provides an analytical model to determine the representative temperature change for the geotechnical design of energy piles. To this end, the expression of the average temperature change corresponding to the average strain of the pile cross-section is firstly derived according to the assumption of strain compatibility. The representative temperature change calculation approach is further proposed by introducing the thermal resistance and heat source model. Comprehensive validation of the proposed model is presented by using experimentally verified numerical simulations. Besides, climatic conditions, heat exchange pipe configurations, and pile diameter on the representative temperature change are studied. The results show that the proposed model is capable of calculating the representative temperature change effectively. Overall, the proposed model provides a reliable approach to determining the representative temperature change used in the geotechnical design of energy piles, and its feature that avoids cumbersome numerical simulations and computing make it have extensive application prospects in the geotechnical design of energy piles.

Keywords: Energy pile; Analytical model; Representative temperature; Geothermal energy

1. Introduction

Energy pile is a hybrid system that integrates heat exchanger pipes of ground source heat pump (GSHP) into the pile foundation[1–3]. Energy pile has the dual function of supporting superstructures and transferring the heat energy between buildings and the surrounding soil. This hybrid system saves drilling costs and underground space in ground-coupled heat pumps (GCHPs)[4].

The thermal load imposed on the energy pile continuously varies with the thermal demand of buildings and superstructures[5]. Because energy piles transfer the energy through the heat carrier fluid and pile body, the temperature distribution of the pile cross-section will produce spatial differences[6]. Therefore, the non-uniform temperature change occurs to the cross-section of the pile. It is noted that the current thermomechanical design methods of energy piles usually assume that temperature uniformly changes over the pile domain[4,7–10]. The assumption is widely adopted because of the simplicity when investigating the thermo-mechanical performance of energy piles. The maximum temperature changes are usually adopted to calculate the thermal strain and stress over the pile domain in simplified design methods as well as many numerical and experimental studies[5,6, 11–27,] . However, as discussed in the studies of Abdelaziz et al[28,29], this method of selecting the uniform temperature changes (i.e., representative temperature change) is debatable.

The defects of the method of selecting maximum temperature changes as representative temperature changes are mainly reflected in two parts. On the one hand, the influence of the non-uniform temperature change on the pile cross-section is ignored, and no guidelines are available to select the design temperature change. In these simplified design methods as well as numerical investigations[7–10,13,26], the pile temperature changes over the pile are considered to be equal everywhere at the same time. In these experimental studies[5,20–24], the temperature changes and thermal strains measured respectively rely on the thermistors and strain gauges installed at specific points of the pile during tests. Since the non-uniform temperature change occurs to the cross-section of the pile, mounting positions of measuring instruments have a

significant influence on test results. Therefore, the influence of non-uniform temperature changes to the thermo-mechanical performance has not been considered in these studies mentioned above. Besides, no explicit and consensual standard is developed to guide the installation of test instruments in the design and study of energy piles. On the other hand, the method selecting the utmost temperature change utilized for the energy pile design is conservative. This method can cause a lack of an accurate description of the thermo-mechanical performance of the energy pile and is prone to over-design[28].

Therefore, this study develops the simplified analytical model to calculate the representative temperature change used in the thermo-mechanical design of energy piles. Firstly, the non-uniform thermal strain of the energy pile cross-section is equivalent by the average thermal strain, and the expression of the average temperature change corresponding to the average strain of the section is derived. Then the concept and calculation method of the representative temperature change for energy pile design is proposed based on the simplify analysis of the the complex heat transfer mechanism inside the energy pile. Secondly, the finite element model is validated by comparing the thermomechanical behavior obtained by the simulations and that obtained by the laboratory model test and field test. And then, the analytical model has been verified by comparison with the results of the finite element method. Then, the influence of critical parameters such as climatic conditions, the layout of heat exchange pipes, and pile diameter on the representative temperature change are investigated. Finally, recommendations for the thermomechanical design of energy piles are provided.

2. Analytical model for representative temperature change in pile

2.1 Average temperature change of the pile cross-section

The load transfer mechanism of the energy pile subjected to coupled thermal and mechanical effects had been studied by Bourne-Webb et al.[30] and Rotta Loria et al.[31]. The thermal stresses of an energy pile under different constraints could be expressed as

$$\sigma_{\mathrm{th}} = E_{\mathrm{pile}}\varepsilon^{\mathrm{th}}{}_{\mathrm{cons.}} = E_{\mathrm{pile}}\left(\varepsilon^{\mathrm{th}}{}_{\mathrm{obs.}} - \varepsilon^{\mathrm{th}}{}_{\mathrm{free}}\right) = E_{\mathrm{pile}}\left(\varepsilon^{\mathrm{th}}{}_{\mathrm{obs.}} - \alpha_{\mathrm{pile}}\Delta T\right) \quad (1)$$

where E_{pile} means Young's modulus for energy piles; α_{pile} is the linear thermal expansion coefficient; ΔT is the temperature change; $\varepsilon^{\mathrm{th}}{}_{\mathrm{free}}$ means thermal strains of energy piles without any constraint; $\varepsilon^{\mathrm{th}}{}_{\mathrm{obs.}}$ is the observed thermal strains of energy piles with constraint; $\varepsilon^{\mathrm{th}}{}_{\mathrm{cons.}}$ is thermal constraint strains of energy piles, which induces observed thermal stresses.

The underlying assumption of the above derivation is that the temperature of the pile cross-sections and depth changes uniformly. However, the non-uniform temperature change could be induced to cross-sections of the pile due to the thermal load continuously varies with the working demand influenced by climate change and other factors. The temperature change of the concrete domain near heat exchanger pipes varies higher than that far away from heat exchanger pipes. Non-uniform variation of temperature will result in the non-uniform strains, i.e., $\varepsilon^{\mathrm{th}}{}_{\mathrm{free\text{-}i}}$, over the pile cross-section. Abdelaziz et al.[29] investigated and discussed the phenomenon by utilizing a two-domain analogy consisting of the pile and soil domains. Based on this method, a three-domain analogy, including the pile, soil, and superstructure domains, is used to explore the interaction in terms of the superstructure, pile, and soil under the non-uniform temperature change, as shown in Fig.1.

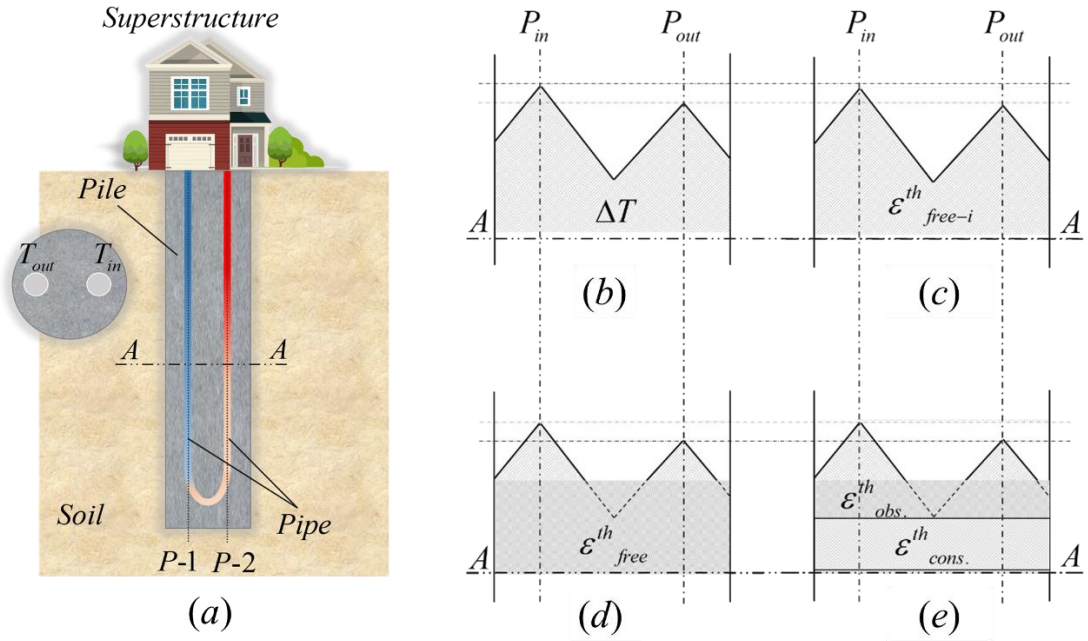

Fig. 1 Three domains controlling the coupled performance of pile: (a) schematic diagram of the energy pile. (b) the temperature change for the energy pile cross-section; (c) local free thermal strain; (d) the average thermal strains; (e) constrain and observed strains (after on the study of Abdelaziz et al.[29])

When the energy pile is free, the non-uniform strains induced by the non-uniform temperature change distribute variously to the cross-section of the pile, as shown in Fig. 1(b) and Fig. 1(c). Nevertheless, despite the non-uniform temperature changes and the resulting non-uniform free thermal strains, any cross-section along the pile will meet the strain compatibility requirements resulting in uniform deformation. That is to say, the non-uniform strains are adjusted through the strain compatibility to achieve a uniform strain and deformation of the pile cross-section, as represented by the average thermal strain, i.e., $\varepsilon^{\text{th}}_{\text{free}}$. The process is illustrated in Fig. 1(c) and Fig. 1(d). The average thermal strain can be written as

$$\varepsilon^{\text{th}}_{\text{free}} = \frac{\int_{A_{\text{pile}}} \varepsilon^{\text{th}}_{\text{free-i}} da}{A_{\text{pile}}} \tag{2}$$

where A_{pile} is the pile section area. For the pile area near heat exchanger pipes, local thermal strains ($\varepsilon^{\text{th}}_{\text{free-i}}$) are more significant than the average thermal strain ($\varepsilon^{\text{th}}_{\text{free}}$), and the extra part would be blocked because of strain compatibility. Similarly, for the

pile area where the local thermal strains are lower than the average thermal strain, the strain difference would be replenished because of the strain compatibility.

For energy piles constrained by superstructures and surrounding soil, the average thermal strain is bounded by the external resistance. Some of them transform to constraint strains ($\varepsilon^{\text{th}}_{\text{cons.}}$), which result in thermal stresses, as shown in Fig. 1(e). Therefore, the sum of constraint and observed thermal strains is equal to the average thermal strain of the free pile.

The continuously varying thermal load induces the non-uniform temperature change and strain of the pile cross-section. The average thermal strain uniformly distributes on the cross-section of the pile because of strain compatibility. The assumption is the basis of one-dimensional methods previously proposed to study the thermo-mechanical performance of the energy pile subjected to coupled effects[7–10]. In these methods, the average thermal strains are the key to trigger the interaction of soil- and superstructure-pile. According to the study mentioned above[29], the average thermal strain could be expressed by a corresponding average temperature change ($\Delta T_{\text{average}}$).

$$\varepsilon^{\text{th}}_{\text{free}} = \alpha_{\text{pile}} \Delta T_{\text{average}} \tag{3}$$

The local thermal strain ($\varepsilon^{\text{th}}_{\text{free-i}}$) could also be expressed by corresponding local temperature change (ΔT_i) according to Eq.(4)

$$\varepsilon^{\text{th}}_{\text{free-i}} = \alpha_{\text{pile}} \Delta T_i \tag{4}$$

Assuming that the pile thermal expansion coefficient is temperature independent and replacing $\varepsilon^{\text{th}}_{\text{free}}$ and $\varepsilon^{\text{th}}_{\text{free-i}}$ from Eq. (3) and (4), the Eq. (2) could be simplified and the average temperature change for the pile section could be written as

$$\Delta T_{\text{average}} = \frac{\int_{A_{\text{pile}}} \Delta T_i da}{A_{\text{pile}}} \tag{5}$$

2.2 Temperature response of the pile wall and inside the pile

To calculate the representative temperature change, it is essential to get the actual

temperature distribution of the pile cross-sections. In the design and study of GSHPs and energy piles, the infinite line source model (ILS) is widely utilized to calculate the temperature of the borehole wall or pile wall[32]. The ILS model regards the borehole or the pile as the infinitely long constant line heat source and performs one-dimensional unsteady heat transfer analysis in the surrounding soil. However, the pile diameter is more significant than that of the borehole, and the energy pile depth is far from infinite. Then researchers have proposed the finite line source model (FLS)[33] based on the concept of infinite line heat source model. The FLS model assumes the ground as a constant temperature boundary condition and regards the pile as finite length; thus, it can describe the vertical spatial difference of the surrounding soil temperature field with depth. In this model, a virtual heat source based on the classical line source theory is introduced, and the Green's function is utilized to process the temperature responses generated by the finite line heat source in the semi-infinite soil. The analytical expression is shown as

$$\Delta T\left(r,z,t\right)=\frac{q}{4\pi\lambda_{\text{soil}}}\int_0^H\left[\frac{erfc\left[\frac{\sqrt{r^2-\left(z-h\right)^2}}{2\sqrt{\alpha t}}\right]}{\sqrt{r^2-\left(z-h\right)^2}}-\frac{erfc\left[\frac{\sqrt{r^2-\left(z+h\right)^2}}{2\sqrt{\alpha t}}\right]}{\sqrt{r^2-\left(z+h\right)^2}}\right] \tag{6}$$

where r is the radial distance; z is the depth below the ground; t is the duration of heat transfer; q is the heat flow of per unit pile depth; λ is the soil thermal conductivity; α is the thermal diffusion coefficient of the soil; $erfc\left(x\right)$ is the error function complement.

The FLS model can analyze temperature responses of pile wall versus time and predict the change of ground temperature field induced by the long-term operation, which is the key to calculate the representative temperature change. The heat transfer mechanism inside the pile will be analyzed in section 2.3. In addition, it is noted that the underlying assumption of Eq. (6) is that the heat flow (i.e., q) provided by the energy pile is time-independent. However, the heat extraction or injection by energy piles

dynamically varies with the building's thermal load in the actual operation. Thus, the FLS model gets a lack of much precision in calculating the temperature change of the pile subjected to the dynamic thermal load. Yavuzturk[34] and Bernier et al.[35] proposed a procedure to perform the time-by-time temperature response with a traditional constant heat source model. Therefore, in this study, the procedure is introduced into the traditional FLS model to consider the impact of the variable heat flow on energy piles.

According to the procedure of Yavuzturk[34] and Bernier et al. [35], the effect of the variable heat flow can be presented by introducing the underlying step pulse. The heat extraction or injection is considered as constant in piece-wise and superimposed in time as a series of step pulses. Therefore, the solution of the FLS model could be utilized to represent transient temperature responses generated in the pile wall subjected to the continuously various thermal load in this way. The process is graphically demonstrated in Fig. 2. The continuously varying thermal load is divided into a series of step pulses, each of which produces a temperature response to the pile wall, as shown in Fig. 2. Thus, the total temperature responses of the pile wall at a particular time can be obtained by superimposing all the previous temperature responses induced by step pulses. Mathematically, the superimposition of the pile wall temperature response at the end of the t_n time could be expressed as

$$\Delta T_{\text{pile-wall}}\left(z,t\right)=\sum_{i=1}^{n}\frac{q_i-q_{i-1}}{4\pi\lambda_{\text{soil}}}\int_0^H\left[\frac{erfc\left[\frac{\sqrt{r_{\text{pile}}{}^2-\left(z-h\right)^2}}{2\sqrt{\alpha\left(t_{\text{n}}-t_{i\text{-}1}\right)}}\right]}{\sqrt{r_{\text{pile}}{}^2-\left(z-h\right)^2}}-\frac{erfc\left[\frac{\sqrt{r_{\text{pile}}{}^2-\left(z+h\right)^2}}{2\sqrt{\alpha\left(t_n-t_{i-1}\right)}}\right]}{\sqrt{r_{\text{pile}}{}^2-\left(z+h\right)^2}}\right] \quad \textbf{(7)}$$

where r_{pile} is the radius of the pile. It is noted that t_0 and q_0 equal zero in initial. As shown in Eq. (7), the FLS model with temporal superposition could be used to calculate the temperature variations of the pile-wall subjected to dynamic thermal loads. Also, it can well reflect the transient temperature responses generated in the energy pile wall under continuously various thermal loads.

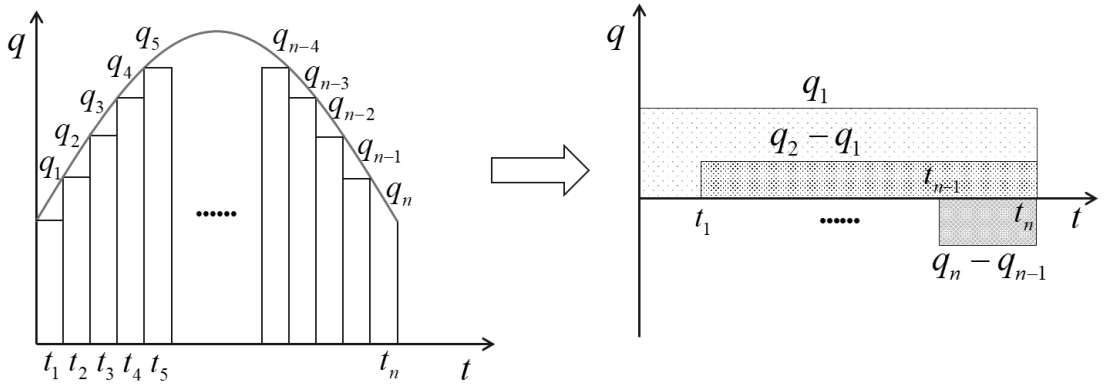

Fig. 2 Superposition of piece-wise linear step heat inputs in time

As mentioned above, the key to calculate the representative temperature is to get the distribution of the local temperature change for the energy pile cross-section, i.e. ΔT, which could be calculated by the pile wall temperature obtained by using the FLS model with temporal superposition and heat transfer model inside the pile. Next, the detailed derivation process of the heat transfer model inside the pile will be given according to the basic principles of heat transfer.

According to the study of Gu et al.[36], the heat exchanger pipes could be expressed by an equivalent diameter pipe for the thermal analysis of the energy pile, as shown in Fig. 3. The equivalent diameter can be written as

$$D_{\mathrm{eq}} = \sqrt{n} D \tag{8}$$

where D is the outer diameter of the heat exchanger pipes; n denotes the number of the legs of the heat exchange pipes.

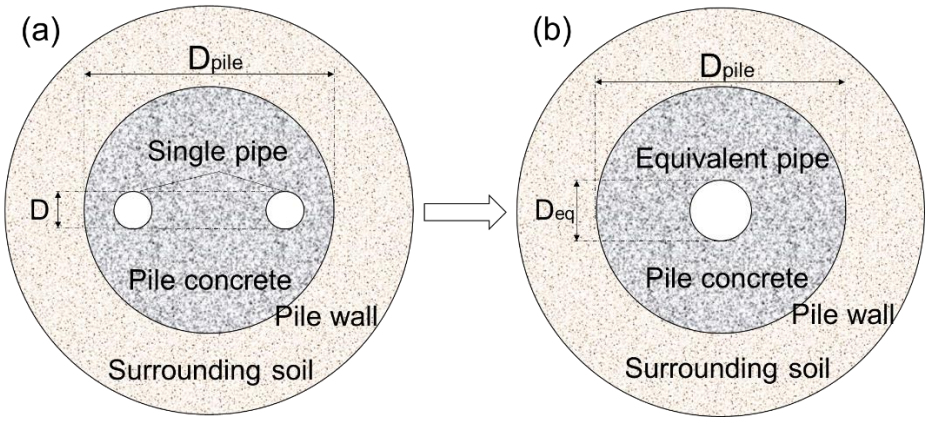

Fig. 3 Simplification of energy pile; (a) true pile; (b) equivalent pile

The concept of the thermal resistance could present the radial heat transfer

mechanism over the pile cross-section. Assume that heat exchange pipes are in complete contact with the concrete. The heat transfer process could be divided into three phases consisting of the heat transfer from heat carrier fluid to the heat exchanger pipe wall, the heat conduction of heat exchanger pipes, and concrete, as shown in Fig. 4. The three phases correspond to the thermal resistance named R_{fluid} , R_{pipe} and R_{concrete} , respectively. The r_{eq} in the figure means the radius of the equivalent heat exchanger pipe.

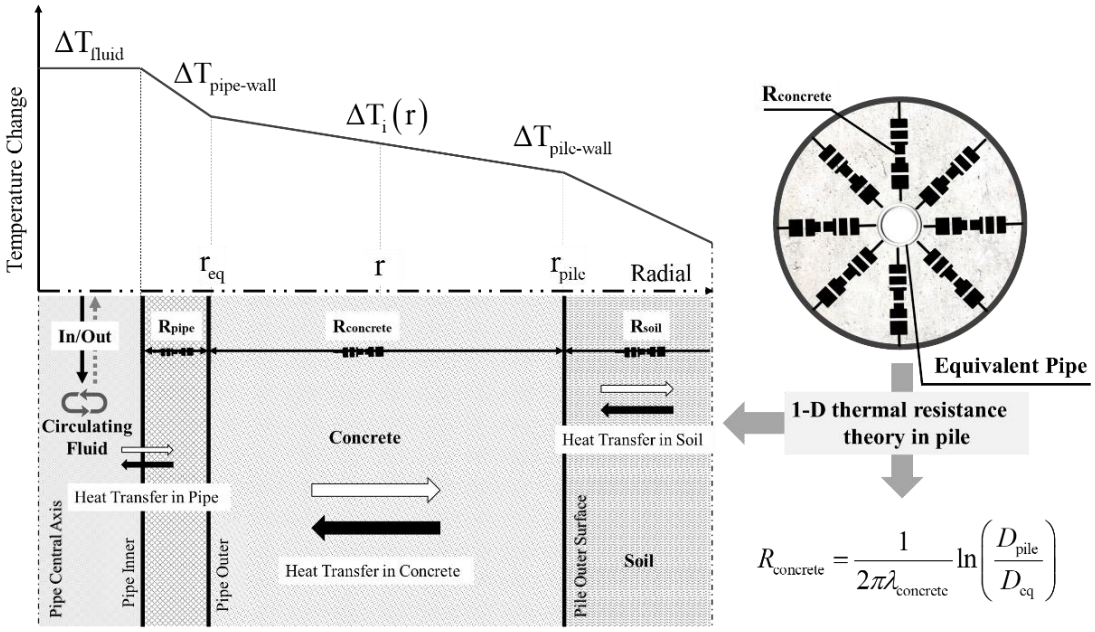

Fig. 4 1-D Heat transfer process of the pile cross-section

It is worthy to note that the mechanical load on the heat carrier fluid and heat exchanger pipes could be neglected compared to the concrete. Thus, the representative temperature change means the average temperature change of the energy pile section. The relationship between the pile-wall and heat exchanger pipe outer wall temperature could be expressed by the Eq. (9), according to the heat transfer theory.

$$\Delta T_{\text{pipe-wall}} = \Delta T_{\text{pile-wall}} + qR_{\text{concrete}} \tag{9}$$

where the temperature change at the pile-wall could be calculated by using Eq. (7) and R_{concrete} can be calculated by the Eq.(10), according to the study published previously[37].

$$R_{\text{concrete}} = \frac{1}{2\pi\lambda_{\text{concrete}}} \ln\left(\frac{D_{\text{pile}}}{D_{\text{eq}}}\right) \tag{10}$$

where $\lambda_{\text{concrete}}$ is the pile thermal conductivity coefficient; D_{pile} is the pile diameter.

2.3 Calculation of the representative temperature change of the pile

According to the content about heat transfer model inside the pile discussed in section 2.1, the local temperature change at any location in the energy pile cross-section at the end of the t_n time could be written as

$$\Delta T_i\left(r, t_n\right) = \frac{q_n R_{\text{concrete}}}{r_{\text{eq}} - r_{\text{pile}}}\left(r - r_{\text{pile}}\right) + \Delta T_{\text{pile-wall}} \tag{11}$$

Substituting for the local temperature change from Eq.(11), the Eq. (5) can be expressed as

$$\Delta T_{\text{average}}\left(t_n\right) = \frac{1}{\pi\left(r_{\text{pile}}^2 - r_{\text{eq}}^2\right)} \int_0^{2\pi} \int_{r_{\text{eq}}}^{r_{\text{pile}}} \frac{q_{\text{n}} R_{\text{concrete}}}{r_{\text{eq}} - r_{\text{pile}}}\left(r - r_{\text{pile}}\right) + \Delta T_{\text{pile-wall}} dr d\theta \tag{12}$$

The average temperature change distribution, along with the pile depth, will be different because of the underlying assumption of the FLS model[32]. The temperature change (i.e., representative temperature change) used in the thermo-mechanical design of the energy pile should be the most representative among these average temperature changes. In engineering practice, the integral average temperature change along with the depth is usually adopted in the design and study of the energy pile or vertical geothermal heat pumps. Therefore, the representative temperature change ($\Delta T_{\text{representative}}$) could be expressed as

$$\Delta T_{\text{representative}} = \frac{1}{H} \int_0^H \Delta T_{\text{average}}\left(z, t_{\text{n}}\right) dz \tag{13}$$

Overall, the flowchart for the model of calculation of the representative temperature change is illustrated in Fig. 5. As it can be seen, by introducing the finite line heat source model with temporal superposition and the internal heat transfer analysis of the energy pile based on the thermal resistance theory, the specific values of the required representative temperature can be easily calculated.

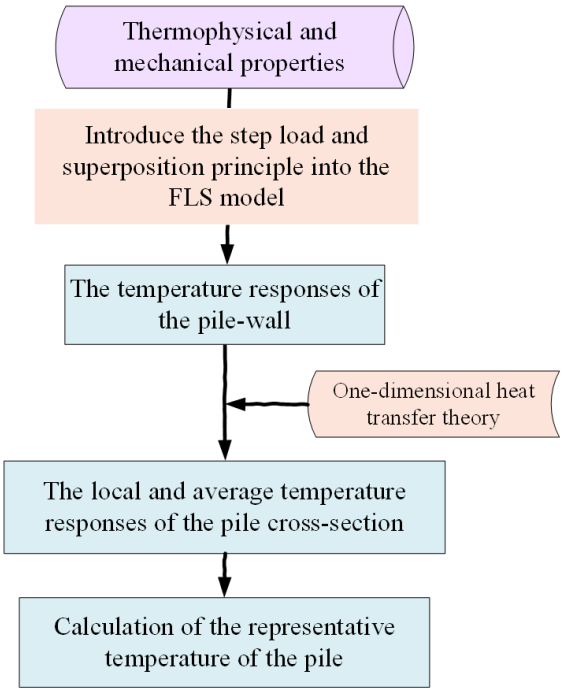

Fig. 5 Flowchart of the model to calculate the representative temperature change

3. A numerical model for verifying the proposed analytical model

The finite element (FE) model is utilized to validate the proposed analytical model in this section. The numerical simulation is performed on the finite element software ABAQUS[38].

3.1. Mathematical formulation

In this study, the heat transfer in porous materials theory is utilized, and the heat transfer mode is conduction. The energy conservation equation is

$$\rho c_p \frac{\partial T}{\partial t} - \nabla \cdot \left(\lambda \nabla T \right) = 0 \tag{14}$$

where ρ represents the density; c_p is the specific heat; t is heat transfer time; λ is thermal conductivity; ∇ is the gradient. It is worth noting that the thermal properties of the surrounding soil and piles are assumed to be temperature independent.

In the process of thermo-mechanical coupling analysis, the equilibrium equation can be expressed as

$$\nabla \cdot \sigma_{ij} + \rho g_i = 0 \tag{15}$$

where g_i represents the gravity vector; ∇ denotes the divergence; σ_{ij} is the total stress tensor, and it can be written as

$$\sigma_{ij} = C_{ijkl}\left(\varepsilon_{kl} + \alpha\delta_{kl}\Delta T\right) \tag{16}$$

where C_{ijkl} is elastic stiffness tensor; ε_{kl} denotes the total strain tensor; α is the linear thermal expansion coefficient; δ_{kl} represents the identity matrix; ΔT is the temperature variation.

3.2. Model geometries and boundary conditions

The model size and schematic diagram of model geometry are shown in Table 1 and Fig. 6, respectively. The numerical model is solved with the 3D domain, which is meshed by tetrahedral grids to reduce the total mesh number and simultaneously get more accurate results. Due to the heat exchange pipes and pile body are the key to investigate the heat transfer, the mesh of this domain is added. Meanwhile, the mesh near the elbow is added due to the irregular shape of the domain near the elbow of heat exchanger pipes.

Table 1 Model geometries

Term	Outer diameter	Depth	Wall thickness
Heat exchanger pipe	32mm	10m	6mm
Pile	1m	10m	---
Heat carrier fluid	20mm	10m	---
Surrounding soil	20m	20m	9.5m

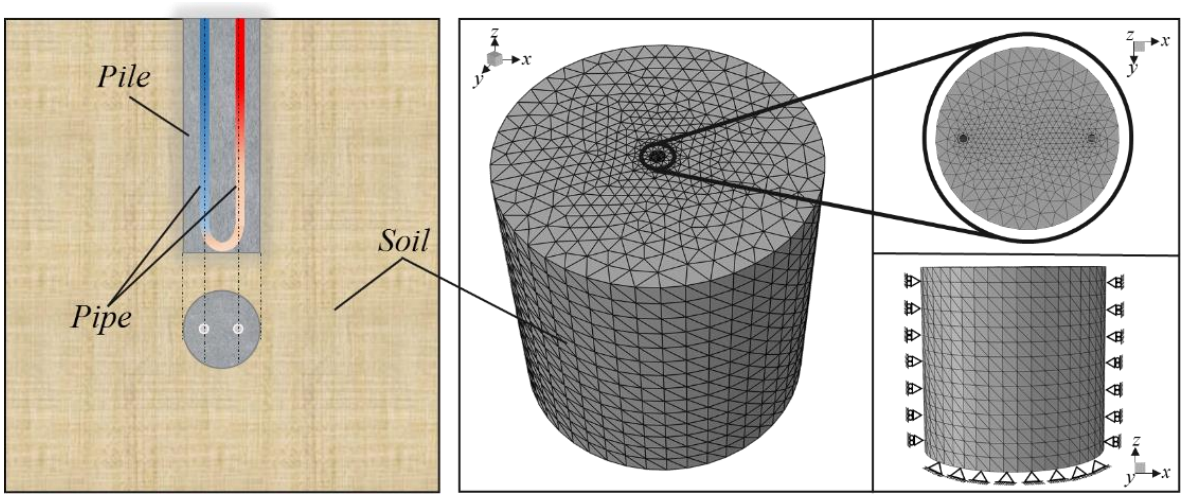

Fig. 6 The schematic diagram of model geometry and thermo-mechanical boundary conditions

In the thermal analysis, the initial temperature of the model is assumed to be 15 ℃. The surface thermal boundary conditions are set to external air temperature. There is a terrestrial surface flux of 0.0544 W/m^2 to be imposed on the bottom boundary. In the lateral boundaries, adiabatic conditions are considered. It is noted that these thermal boundaries have been successfully employed by Rammal et al.[19] to model the long-term thermomechanical behavior considering different thermal solicitations. In the thermomechanical analysis, pinned boundary restrictions are imposed on the base of the model. Thus, both horizontal and vertical displacements are blocked. Roller boundary restrictions are applied to the lateral sides of the model that prevent horizontal displacements on the sides. In addition, the thermal load as the heat source evenly distributes in the heat carrier fluid domain simulated by an equivalent solid in the heat exchanger pipes, as shown in the Eq.(17) [28,39].

$$Q_{\text{applied}} = \frac{Q_1}{n\pi r^2} \tag{17}$$

where Q_{applied} is the thermal load applied to the heat carrier fluid domain; r is the inner diameter of the heat exchange pipe; n is the number of the heat exchange pipes.

3.3. Material properties

The material properties of the heat exchange pipe, pile, and soil have been

successfully employed by Olgun et al.[5] and Abdelaziz et al.[28] to model the non-uniform temperature variations of energy pile cross-sections and thermomechanical behavior of energy piles, respectively. Table 2 summarises the thermo-physical properties considered for the simulations.

Table 2 Material properties utilized for the finite-element analysis[5,28].

	Soil	Pile	Heat exchanger pipes
Density(kg/m^3)	1910	2500	960
Thermal conductivity (W/m K)	2.00	1.50	0.39
Heat capacity (J/kg K)	1500	1000	2300
Poisson's coefficient	0.3	0.2	0.38
Elastic modulus (MPa)	73	20,000	950
Linear thermal expansion coefficient	5×10^{-6}	12×10^{-6}	120×10^{-6}
Friction angle	31°	---	---
Cohesion (kPa)	3	---	---

3.4. FE model for thermal and thermomechanical analysis

3.4.1 Thermal analysis

The energy pile considered in this study is under the sinusoidal balanced thermal load of one year (i.e., mild climatic condition), as shown in Fig. 7. It can be expressed as[39].

$$Q_1 = A\sin\left(\frac{2\pi}{P}t + B\right) \tag{18}$$

where P is one year; t is time; A is the maximum amplitude of the thermal load; B is the coefficient of the equation. The thermal process in terms of the heat convection of the inner heat exchanger pipe and the heat carrier fluid, and the heat conduction in the heat exchanger pipes wall, are all considered in the Eq.(14) [28,29]. 80W/m is selected as the limit of typical heat exchange capacity between the energy pile and surrounding soil[40,41]. The pile is applied to given heating or cooling thermal load for six months, respectively, as adopted by Abdelaziz et al.[28]and Lazzari et al.[39].

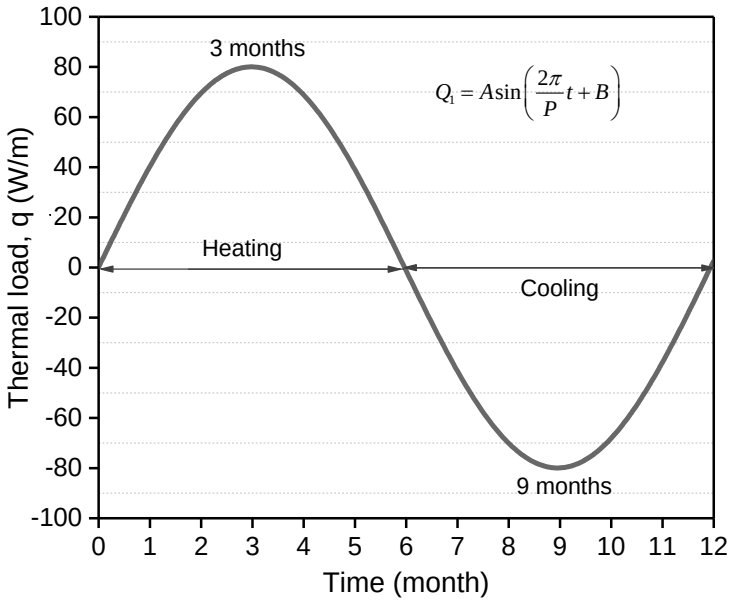

Fig. 7 Balanced annual thermal load

3.4.2 Thermomechanical analysis

The thermo-mechanical coupling process is realized by the sequential coupling code of ABAQUS[38], which can be classified as a weak thermomechanical coupling method. This means that the temperature field is independent of the state stress. Then the results of heat transfer analysis are regarded as initial thermal conditions to be imported into the mechanical analysis model[38]. This study assumes the pile to be in place[19,42,43] and gains the initial stress state by imposing gravity force to the model domain. The mechanical performance of the pile and surrounding soil are simulated by the linear elasticity and Mohr-Coulomb failure criterion, respectively. Besides, in order to simulate the interaction between the surrounding soil and the energy pile, the Coulomb friction model and the hard contact are adopted respectively in the tangential and vertical direction between the pile and surrounding soil. It is noted that hard contact means that when the pile-soil surface is in touch, the two contact surfaces can transmit contact pressure. When the pile-soil contact pressure becomes zero or negative, the constraint of the contact surface is released.

3.5. Comparison between the numerical results with experimental observations

3.5.1 Comparison with model test results

This section verifies the feasibility of this thermomechanical coupling method by model test conducted at Dalian University of Technology (DUT). Our research group has designed an energy pile experimental system containing multi-sensing technologies that can accurately collect multiple parameters during the operation of the energy pile, as shown in Fig.8[44]. Through using the geometry and relevant physical properties of the experimental model, a corresponding numerical model composed of tetrahedral meshes was established to compare the gap between the experimental and analytical values. The relevant parameters of the model experiment are as follows: effective pile length 0.7m, pile diameter 36mm; pile body concrete elastic modulus is 6.7Gpa, thermal expansion coefficient is 18×10^{-6} /℃, weight is 24 kN/m3; the soil around the pile is Fujian standard sand, the internal friction angle is 31 °, the unit volume weight is 17 kN/m3. In the model test, the pile top has only a loading device with a deadweight of 60 N, and the pile top displacement is not limited. Three thermal cooling cycles with a target temperature variation ΔT=10 ℃ are imposed on the pile by two hours thermal operation. It is noted that the thermal operation is stopped for five hours after each thermal cycle to restore the pile temperature to the laboratory temperature.

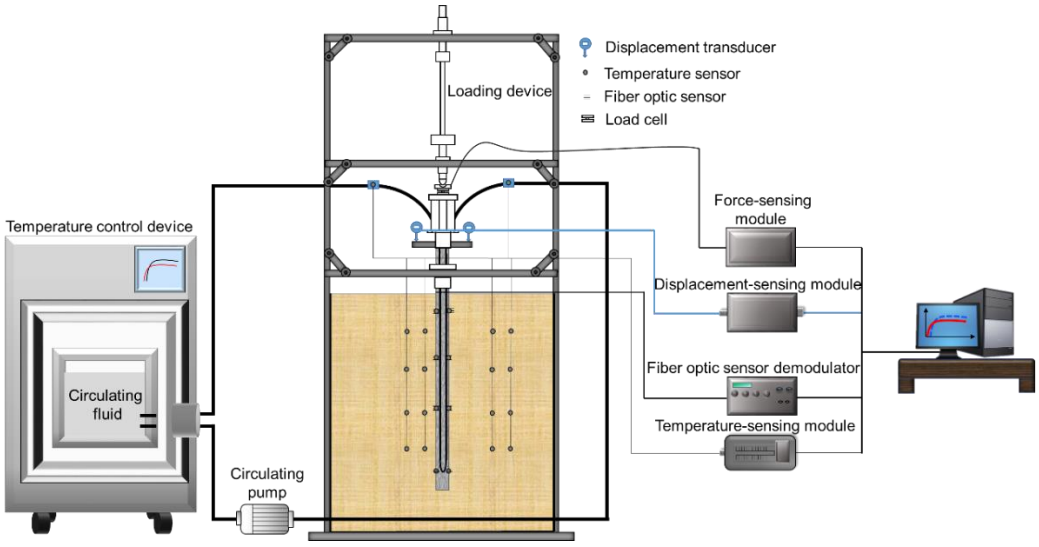

Fig. 8 Energy pile experimental system containing multi-sensing technologies

Fig.9 illustrates the comparison results of experimental and numerical thermal stress. It can be seen that the simulated thermal stress gradually increases along with the pile depth, and reaches the maximum value at 0.45m, and then gradually decreases. The distribution of the simulated thermal stress is the same as the model test results. Besides, as the thermal cycles increase, the simulated thermal stress also gradually increases, which is in good agreement with the overall trend of experimental results. Fig.10 shows the variation curve of the test and simulated pile head displacement versus time and thermal cycles. It can be seen from the figure that the simulated value of the displacement and settlement of the pile top is higher than the test value during multiple thermal cycles. As shown in Fig.10(a), the simulated irreversible settlement gradually accumulates with the thermal cycles, but the accumulation rate continues to decrease. After three thermal cycles, an irreversible settlement of 0.144% D (i.e., pile diameter) is generated on the pile head, which is close to the test value of 0.14% D, as presented in Fig.10(b). It is worth noting that although the numerical simulation results and model test results have the same changing trends, there is some difference in value between them. Two reasons may cause this difference. On the one hand, the numerical model does not model the piles above the soil surface to facilitate calculation convergence. On the other hand, although measures have been taken to minimize the friction between the pile and the vertical flange bearing in the model test, there may still be the effect of shaft resistance on the pile head. However, in the numerical simulation, the head is assumed to move freely. In the next section, the applicability and robustness of the finite element method will be further verified and discussed.

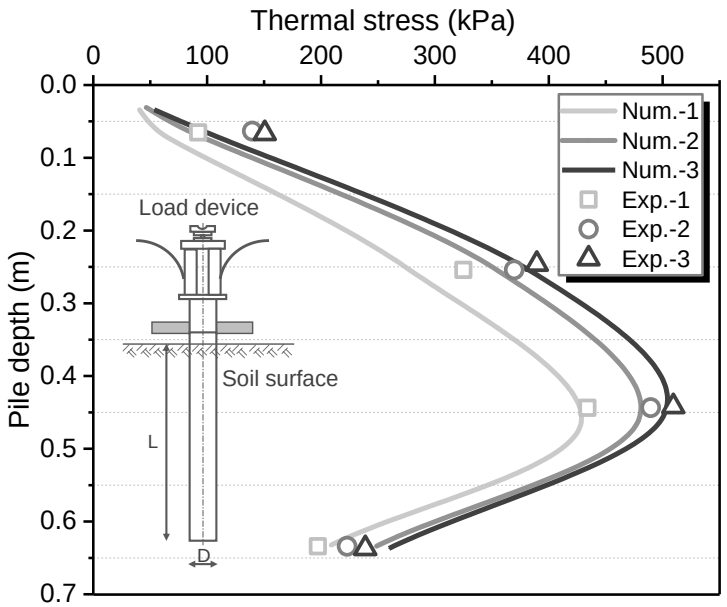

Fig. 9 Results comparison of thermal stress

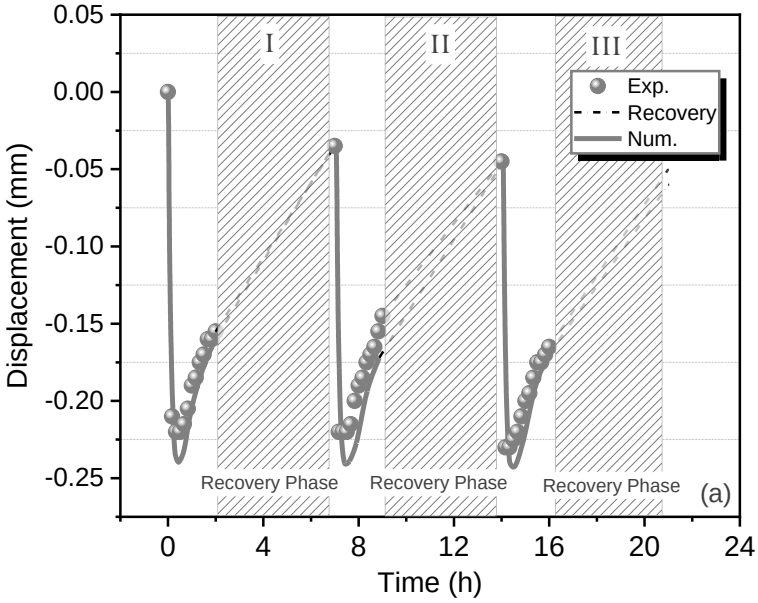

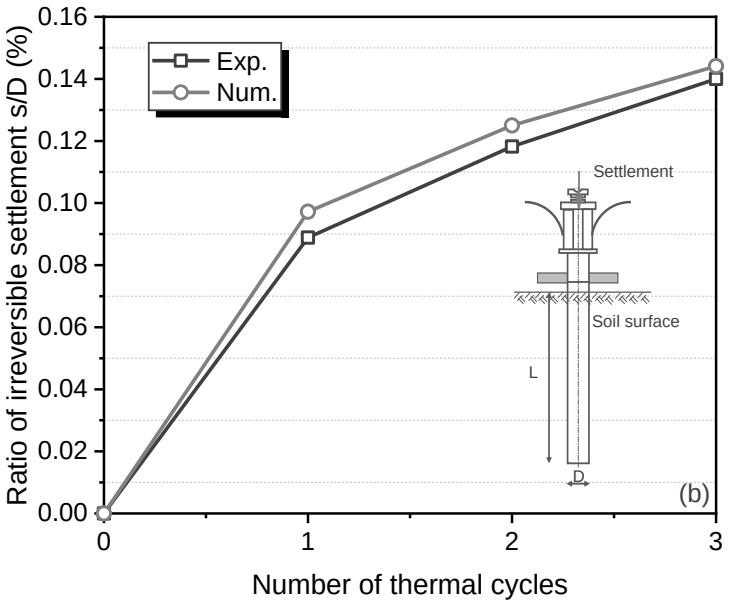

Fig.10 Results comparison of pile head displacement. (a) pile head displacement versus time; (b) irreversible settlement of pile head versus thermal cycles

3.5.2 Comparison with field test results

The simulation results using the finite element model are compared with field test data. The field tests, performed at École Polytechnique Fédérale de Lausanne (EPFL) in Switzerland[16], are employed in this study. The energy pile, with a length of 25.8 m and a design diameter of 0.88 m, is a bored pile with a single U-shaped heat exchange pipe embedded. The elastic modulus of the pile body is 29.2 GPa, and the thermal expansion coefficient is 10^{-5} /℃. The distribution of the on-site foundation soil layer and the parameters used in simulation are shown in Table 3[8,16]. The field test includes seven different tests corresponding to seven successive stages of construction. The results of Test 7 (i.e., conducted at the end of the building construction) are selected for comparison in this study. In Test 7, the mechanical load imposed on the pile is about 1088 kN, and the temperature increment is ΔT=15 ℃.

Table 3 Thermophysical parameters utilized in numerical modeling[16]

Soil layer	Alluvial soil	Alluvial soil	Sandy gravelly moraine	Bottom moraine	Molasse
Density(kg/m^3)	2000	1950	2000	2200	2550
Shear modulus (MPa)	113	113	1000	1400	550-

					2800
Friction angle (°)	30	27	23	27	---
Cohesion (kPa)	5	3	6	20	---
Thermal conductivity (W/m K)	1.8	1.8	1.8	1.8	1.1
Heat capacity (J/kg K)	2.4×10^{-6}	2.4×10^{-6}	2.4×10^{-6}	2.4×10^{-6}	2.0×10^{-6}
Thermal expansion coefficient (/°C)	10^{-5}	10^{-5}	10^{-5}	10^{-5}	10^{-5}

Fig.11 presents the results comparison of the pile vertical stress obtained by experiment and numerical simulation, respectively. It can be seen that the vertical stress gradually decreases along the pile depth when the pile is subjected to mechanical load, and the load is mainly borne by the shaft resistance. Under the thermal operation (i.e., pile temperature change ΔT=15 ℃), thermal stress can be observed obviously due to the fact that the thermal expansion of the pile is partially blocked by the pile-top building and the surrounding soil. The vertical stress of the pile is redistributed under the thermomechanical coupling effect, and the maximum stress appears in the middle area of the pile. Besides, although there is some difference in values between the simulation results and experiment results, the numerical method can accurately simulate the response of the energy pile under the thermomechanical load. Therefore, the fact that the simulations can be agreement well with the results of model tests and field tests shows that the used finite element method can have sufficient reliability and robustness in simulating the thermomechanical response of energy piles.

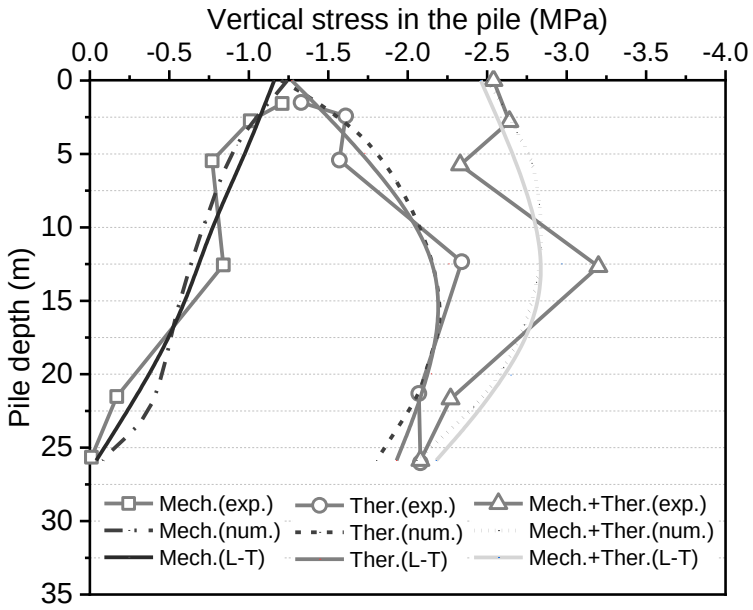

Fig. 11 Results comparison of pile head displacement

In addition, it is worth noting that for the field test mentioned above, this paper also verifies the load transfer method for calculating the thermomechanical response. The load transfer method is proposed by Knellwolf et al. [8] and Chen et al.[10] based on the tranditional load transfer model for pile foundations. This method employs the concept of the neutral plane of energy pile to link the responses of the pile subjected to mechanical load and thermal load and realizes the thermomechanical calculation of the energy pile. The thermophysical parameters and pile dimensions are the same as those mentioned above. Fig. 11 illustrates the comparison between calculations and measurements. In the figure, L-T means the thermomechanical load transfer model. The results show that for the given thermal operation (i.e., pile temperature change ΔT=15 ℃), the calculations and field observations agree well with each other. It is demonstrated that the thermomechanical load transfer model employed in this paper can rationally be utilized to predict the responses of the energy pile subjected to complex loadings.

4. Results and analysis

4.1 Impact of the thermal load forms under different climatic conditions

In order to validate that the analytical model can timely reflect the temperature response of the pile to the transient thermal load, the representative temperature change obtained by the analytical model proposed by this study is compared to that observed at a depth of 5 m by the finite-element model. As shown in Fig.12, the agreement is observed in the results obtained by the analytical model and the finite-element model. As time evolves, the trend of the representative temperature change is consistent with the transient thermal load. This phenomenon indicates that the analytical model can reflect the effect of the transient thermal load on the temperature of the pile in real-time. Also, it is worth noting that the analytical results and finite-element results differ more obvious under heating load than that under cooling load, i.e., the temperature change calculated by the analytical model proposed by this paper is more significant than that approximated by the FE model under the cooling load.

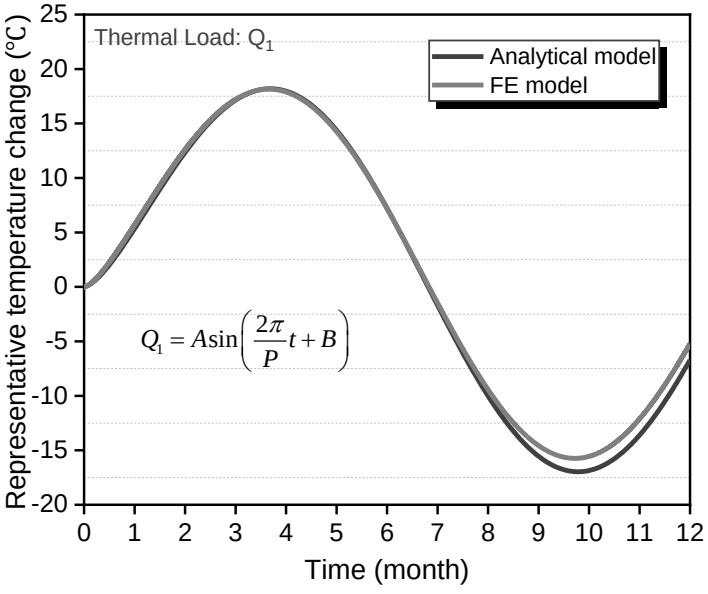

Fig. 12 The validation of the analytical model with temporal superposition subjected to the balanced thermal load

To validate the applicability of the analytical model under different climatic conditions, the other two unbalanced thermal loads are incorporated into the analytical

model and the finite-element model for comparison. The two thermal loads respectively represent the regions where the demand for cooling and heating is unbalanced, i.e., warm and cold climatic conditions[39], as shown in Fig.13. The expressions of these two thermal loads are shown in Eq. (19) and Eq. (20).

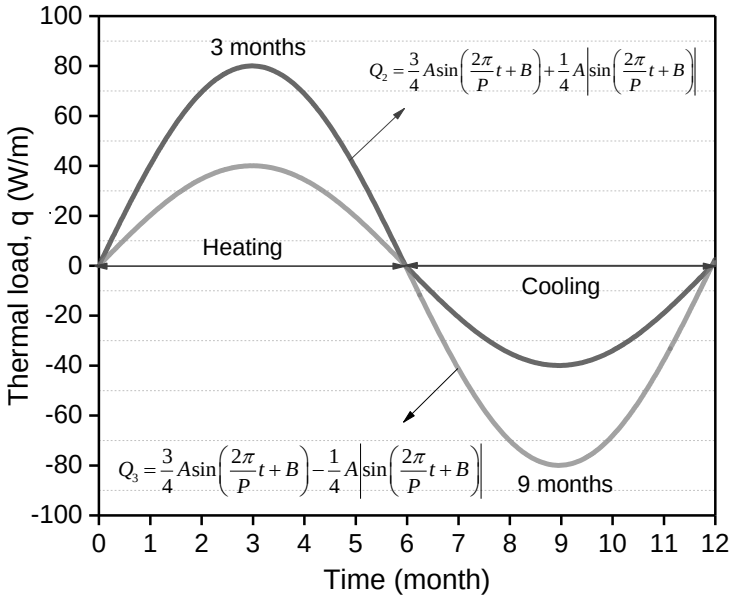

Fig.13 Unbalanced annual thermal load

$$Q_2=\frac{3}{4}A\sin\left(\frac{2\pi}{P}t+B\right)+\frac{1}{4}A\left|\sin\left(\frac{2\pi}{P}t+B\right)\right| \tag{19}$$

$$Q_3=\frac{3}{4}A\sin\left(\frac{2\pi}{P}t+B\right)-\frac{1}{4}A\left|\sin\left(\frac{2\pi}{P}t+B\right)\right| \tag{20}$$

The results are illustrated in Fig.14. The variation trend of the representative temperature change and the thermal load is the same, as shown in the figure. The analytical model can reflect the influence of the transient thermal load on the pile temperature responses in time, which can be used as the basis for the study of pile-soil interaction. As presented in Fig.14, the maximum difference in the temperature change calculated by respectively utilizing the FLS model with temporal superposition and the finite-element model is less than 1℃. Besides, interestingly, the maximum and minimum values of the representative temperature change slightly lag behind that of the thermal loads imposed on the energy pile. This phenomenon can be accounted for that the heat transfer of the heat exchanger pipes, pile body, and the surrounding soil

takes a certain amount of time. When the transient thermal load applied to the heat carrier fluid at a particular moment, the temperature response of the pile is still the combined effect of all the thermal loads before this moment.

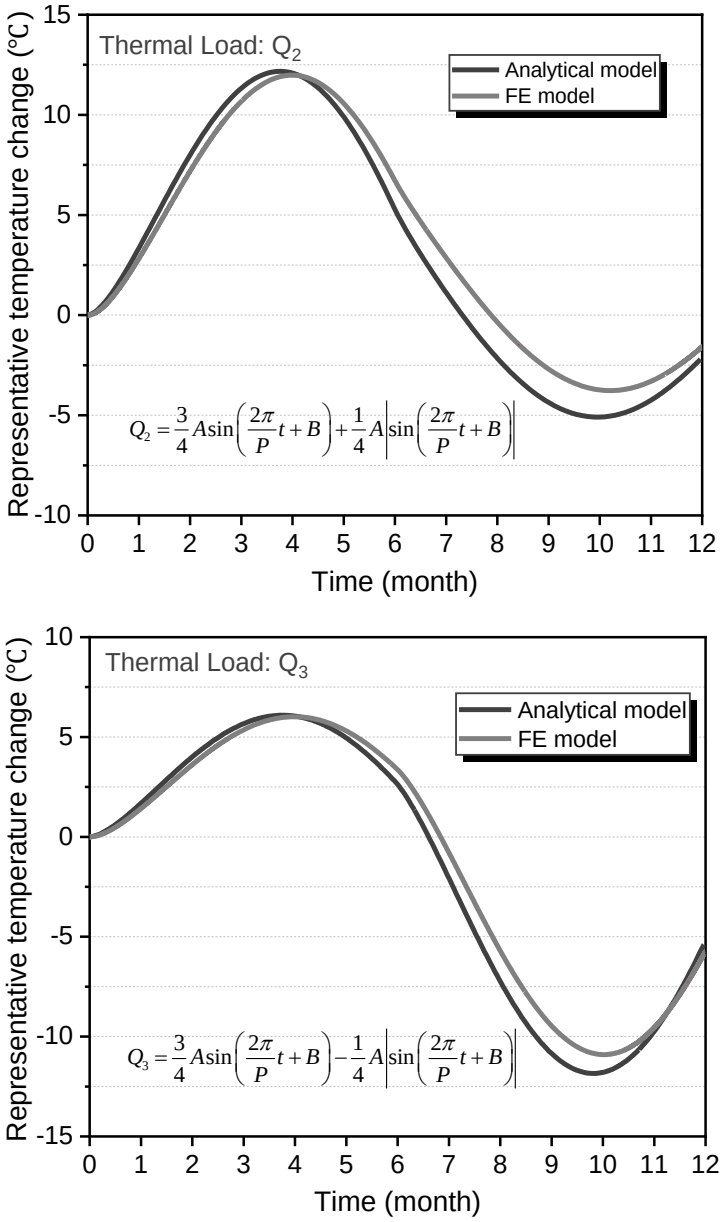

Fig.14 The validation of the analytical model with temporal superposition subjected to the unbalanced thermal load of (a) more heat load than cold load and (b) more cold load than heat load

An interesting phenomenon can be found from the above results. As time goes on, the gap between the representative temperature changes obtained by the analytical model and the representative temperature changes obtained by the numerical simulation

gradually increases. To study whether this difference is related to the order of application of cold and hot loads, we reversed the heat loads representing different climatic conditions to view the comparison results of the analytical model and numerical simulation, that is, Q1, Q2, and Q3 are inverted and applied to the energy pile. Fig.15 shows the representative temperature changes after the sequence of hot and cold loads is reversed. The phenomenon shown in the figure is consistent with the phenomenon without reversal; that is, the gap between the representative temperature changes calculated by the analytical model and the numerical simulation gradually increases over time. Several likely sources of the difference are identified, mostly due to the assumptions adopted by the analytical model: time stepping and heat transfer inside the pile. It can be seen in figures (i.e., Fig.12-15) that the peak time of heat load in the analytical model and numerical simulation is the same. However, the peak time of temperature response in the analytical model is earlier than that in numerical simulation. This is because a fixed time step of one day is used in the analytical model, while a smaller time step is used in the numerical simulation for convergence. The larger time step dramatically reduces the calculation time and reduces the accuracy of the calculation results to a certain extent and result errors, as analyzed in the work of Cullin and Spitler[45]. Additionally, the study of Loveridge and Powrie[46] showed that the assumption of steady-state heat transfer in a pile would overestimate the representative temperature change, which is consistent with the phenomenon observed in this paper. Therefore, the proposed model's steady-state heat transfer assumption also leads to the difference between the analytical model and the numerical simulation.

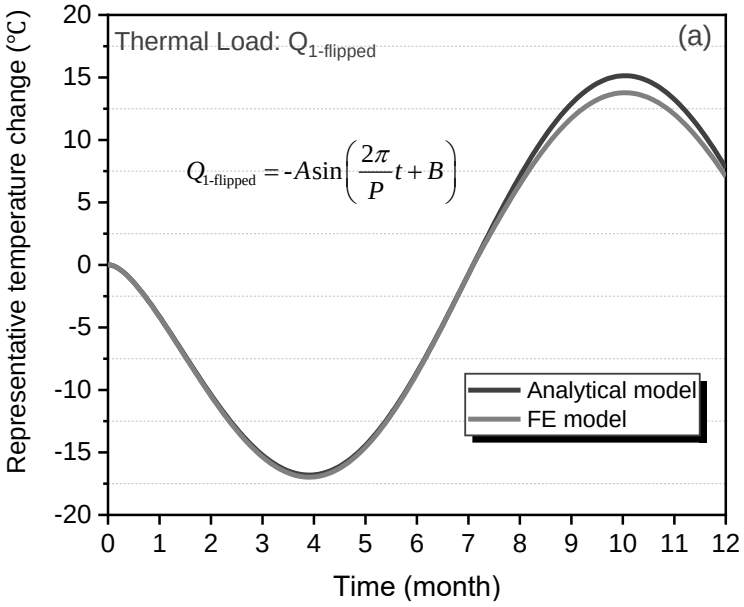
Thermal Load: $Q_{1\text{-flipped}}$
(a)
$Q_{1\text{-flipped}} = -A\sin\left(\frac{2\pi}{P}t + B\right)$
Analytical model
FE model
Representative temperature change (℃)
Time (month)

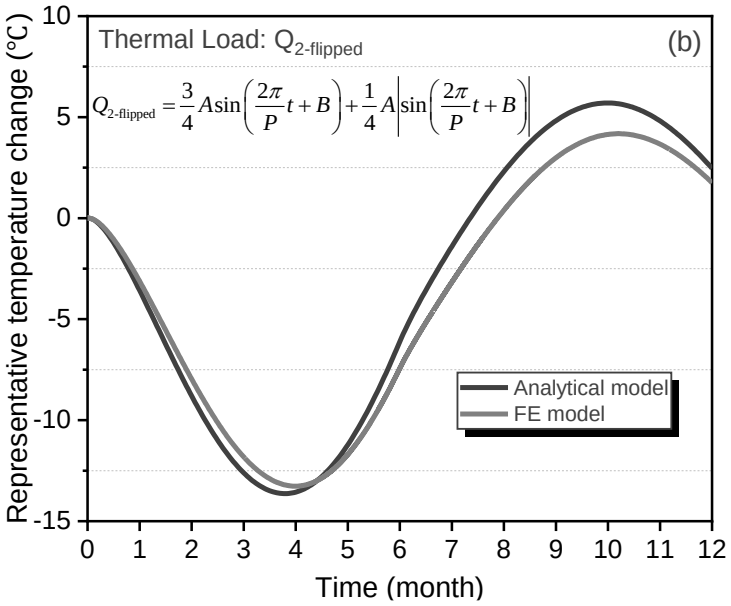
Thermal Load: $Q_{2\text{-flipped}}$
(b)
$Q_{2\text{-flipped}} = \frac{3}{4}A\sin\left(\frac{2\pi}{P}t + B\right) + \frac{1}{4}A\left|\sin\left(\frac{2\pi}{P}t + B\right)\right|$
Analytical model
FE model
Representative temperature change (℃)
Time (month)

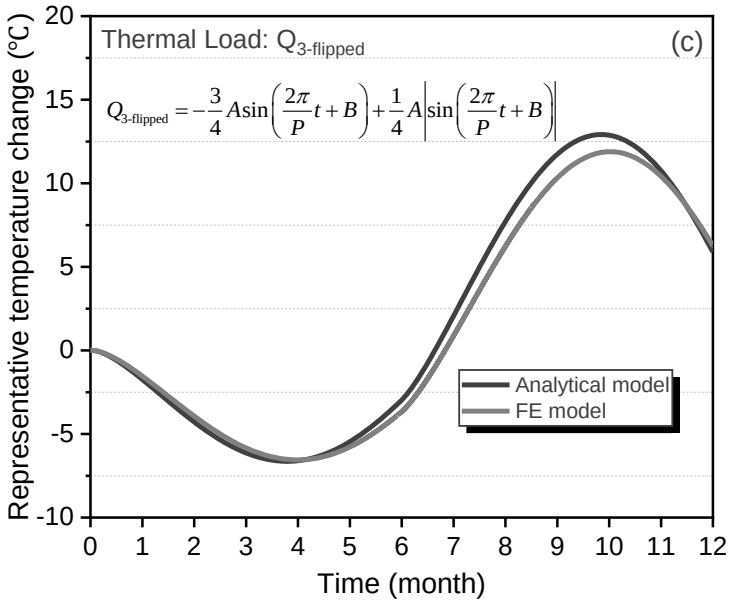

Fig.15 Comparison results between the analytical model and numerical simulation under the reversed thermal loads (a) balanced thermal load, (b) more cold load than heat load and (c) more heat load than cold load

4.2 Representative temperature validation

To verify that the representative temperature change proposed in section 2.3 can meet both strain compatibility, the FE model is utilized to present the temperature distribution over the pile and calculate the stress distribution along with the pile depth. Fig.16, obtained from numerical simulation, illustrates the temperature distribution on the circumference with radii of 0.25R, 0.5R, 0.75R, and 1.0R (i.e., R means pile radius) over the pile cross-section. As shown in Fig.16, the thermal energy is transferred between the heat exchange pipes and concrete, and the closer to the heat exchange pipes, the more dramatic the temperature changes. The temperature change ranges from 12 ℃ to 20.8 ℃, with the weighted average temperature change of 16.4 ℃ in the third month. After subjecting to the thermal loading of the ninth month, the temperature variations range from -10 ℃ to -17.9 ℃ with the weighted average temperature change of -13.95 ℃. These phenomena clearly show the existence of non-uniform temperature changes over the pile cross-section, as described in Section 2.1.

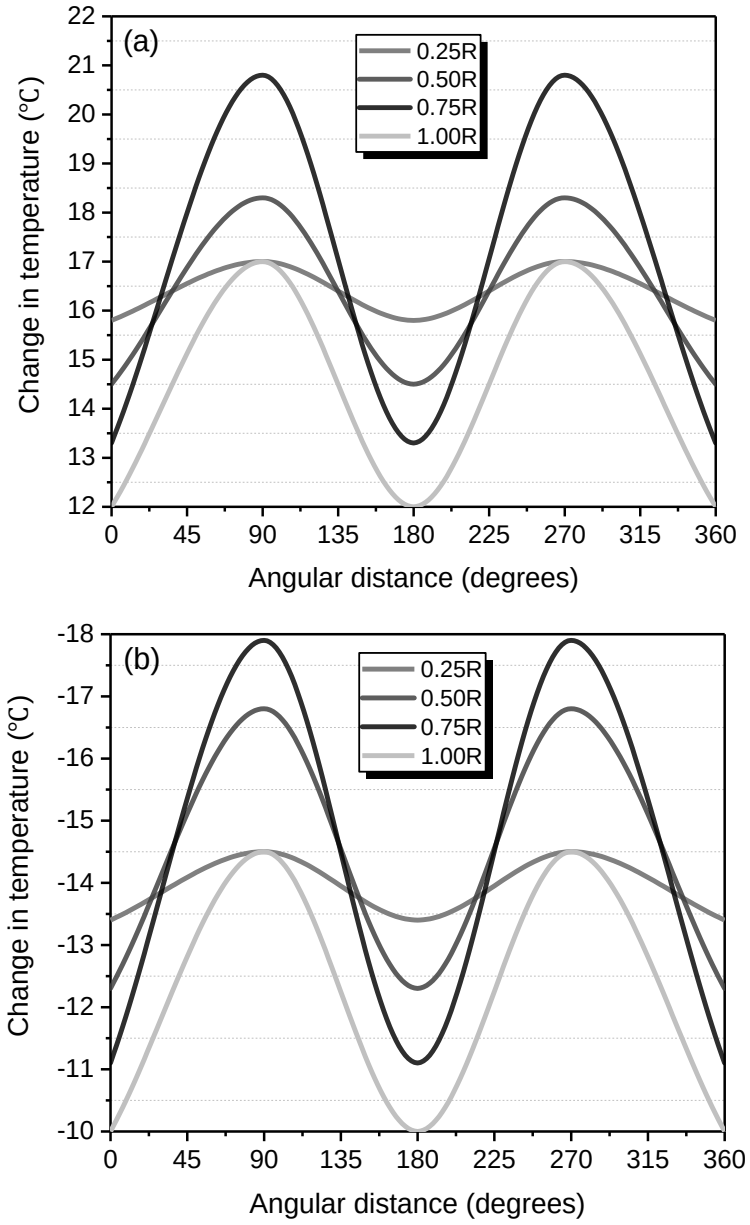

Fig.16 Temperature changes around the circumference with a different radius over the pile cross-section at 5 m depth; (a) subjected to thermal loading of the third month (b) the ninth month.

Figure 17 shows the temperature distribution along with the pile depth under thermal load at different times. As mentioned in section 2.2, the FLS model assumes the ground as a constant temperature boundary condition. These assumptions lead to that the temperature, along with the pile depth, is different. However, when using the one-dimensional method for energy pile design, the critical variable is a representative temperature change. In engineering practices, it has been proposed to utilize the integral

average temperature change along with the pile depth for the energy pile design. The integral average temperature change can consider the unevenness of the pile depth temperature distribution and make the selection of the design temperature change more representative. As presented in Fig.17, the pile average temperature change varies significantly from a pile depth of 2 m to 8 m. In contrast, the temperature changes are small near the pile head and tip. This is because the temperature of the soil surface remains constant during thermal loading. Besides, as time evolves, the difference between the integral average temperature change along with the depth and the average temperature change at intermediate pile depth gradually increases, which may lead to errors in the thermal design for long-term operation of energy piles by using the analytical model proposed by this paper. Thus, further studies would be conducted to improve the analytical model for utilizing in the long-term thermo-mechanical design in the future.

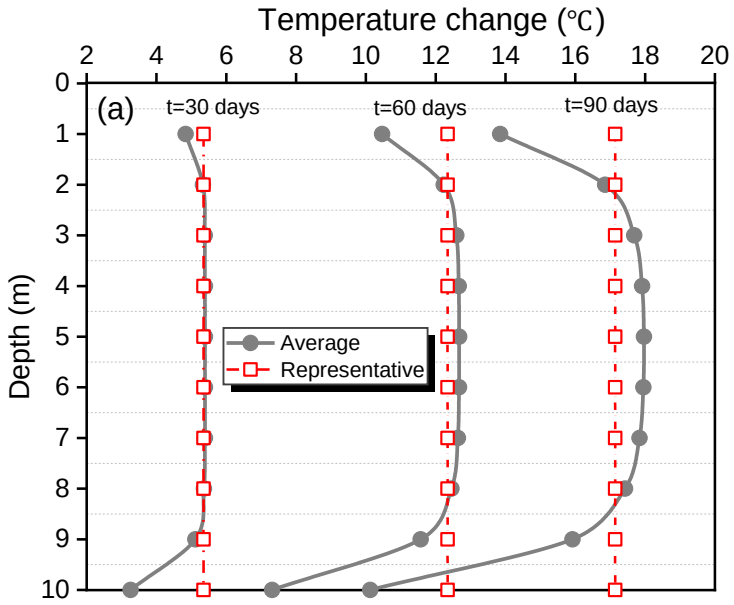

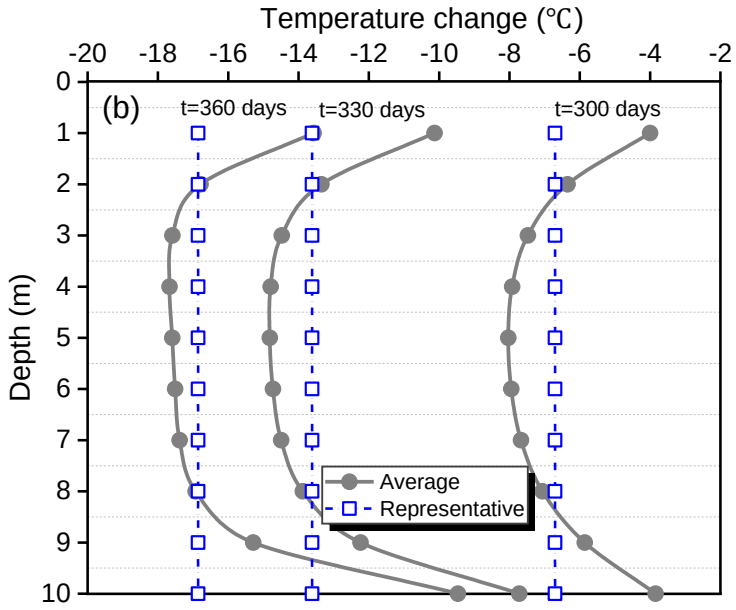

Fig.17 The temperature distribution along with the pile depth subjected to (a) heating (b) cooling.

In order to verify that the proposed analytical model could be utilized to calculate the representative temperature changes for energy piles, the thermal stress calculated by the load transfer method proposed by Knellwolf et al. [8] and Chen et al.[10] is compared to that obtained by the FE model, respectively, as shown in Fig.18. As mentioned in section 2.1, the portion of the constraint-free thermal strain causes thermal stress. Due to the existence of the strain compatibility, the thermal stress of the same section is observed as a uniform and representative value. Furthermore, since the constraints induced by the surrounding soil and superstructures are different at different pile depth, the constraint-free thermal strains of different pile depths are also different. In other words, the thermal stress is unevenly distributed along with the pile depth. When using the one-dimension method, the minimum and maximum average temperature along with the pile depth and the representative temperature are all considered to design initial parameters to calculate the thermal stress, respectively. As shown in Fig.18, the thermal stress obtained by the FE model agrees with the that calculated by one-dimension when incorporating the representative temperature. A similar phenomenon can be observed at other times during thermal loading. The results confirm the rationality of the integral average temperature along with the pile depth as the representative temperature. Also,

it is also validated that as an improvement of the one-dimensional design method of energy pile, the representative temperature change can be utilized to reasonably reveal the thermo-mechanical interaction between the external constraints and the pile. In addition, the difference in Fig.18(b) should be noted. Since the stresses calculated by the analytical and numerical simulation are dependent on the representative temperature change shown in Fig.12, the root cause of the difference between the stresses is the difference between the calculated representative temperatures. The discrepancy of the representative temperature change may be accounted for that the temporal superposition method employed in this study may lead to the accumulation of errors produced by the line heat source model and the internal thermal resistance model inside the pile. That suggests that, in future studies, a heat source model and a thermal resistance model that better fit the actual operating conditions of the energy pile should be used to reduce errors.

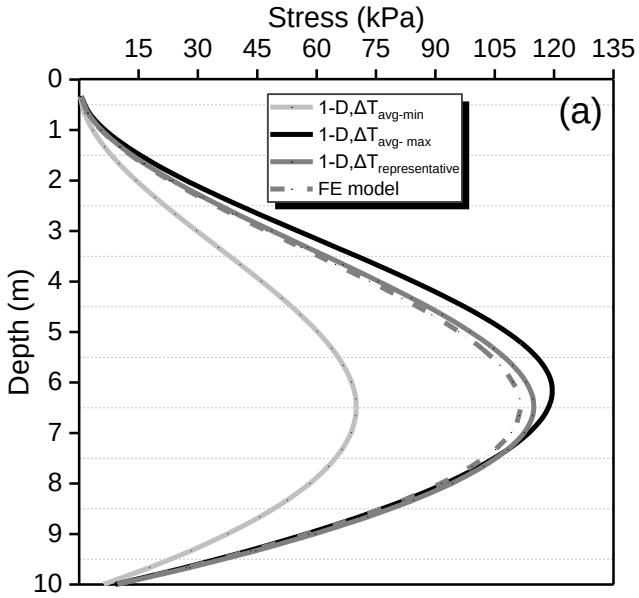

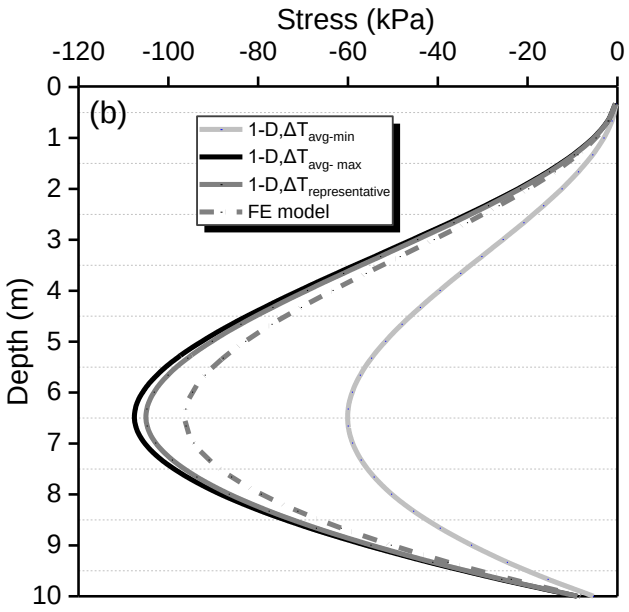

Fig.18 The thermal stress distribution along with the pile depth under (a) heating (b) cooling.

4.3 Effect of the layout of heat exchange pipes

This section aims to study the effect of the layout of the heat exchange pipes on the representative temperature change. It is worth noting that in the calculations in this section, the same total thermal load is used for the calculation of energy piles of different buried pipe types. For this investigation, thermal analysis for four 1m diameter energy piles with different layout of heat exchange pipes is conducted. The balanced thermal loads, presented in Fig.19, are imposed on these four considered piles. The results, shown in Fig.19, indicate that the representative temperature change is positively related to the number of heat exchange pipes. The phenomenon is expected because the pile domain over which the thermal load is imposed increases with the number of heat exchange pipes. Besides, according to Eq. (8) and (10), all pipes are equivalent to one for calculation. For a given pile diameter, the more the number of heat exchange pipes, the larger the area of the equivalent pipe, the smaller the concrete area, and the smaller the corresponding thermal resistance. Thus, the energy pile with a large number of heat exchange pipes is more comfortable to transfer heat, and the higher the representative temperature calculated.

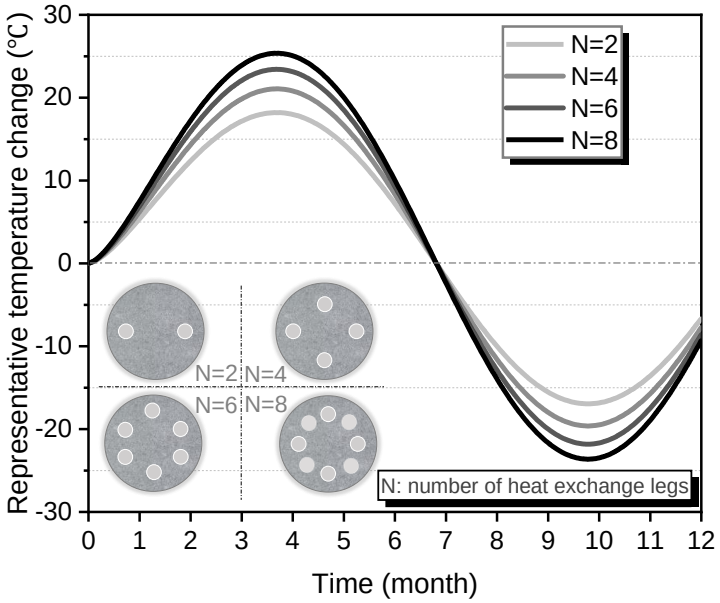

Fig.19 Representative temperature change for energy piles with different layout of heat exchange pipes

4.4 Effect of the pile diameters

In this section, we studied the impact of the pile diameter on the representative temperature change. Three energy piles, with different diameters of 0.5m, 0.7m, and 1.0m, are established with the same condition of two heat exchange pipes. The results, shown in Fig.20, indicate that the representative temperature change decreases with the pile diameter increasing. The phenomenon may be caused by the pile domain on which the thermal load is imposed unchanged while the pile diameter increases. Also, as mentioned in Eq. (10), the increase of the pile diameter makes the relative thermal resistance of the pile concrete more significant. Thus, the efficiency of heat transfer between the thermal carrier fluid and the surrounding soil decreases, resulting in the lower of the calculated representative temperature change.

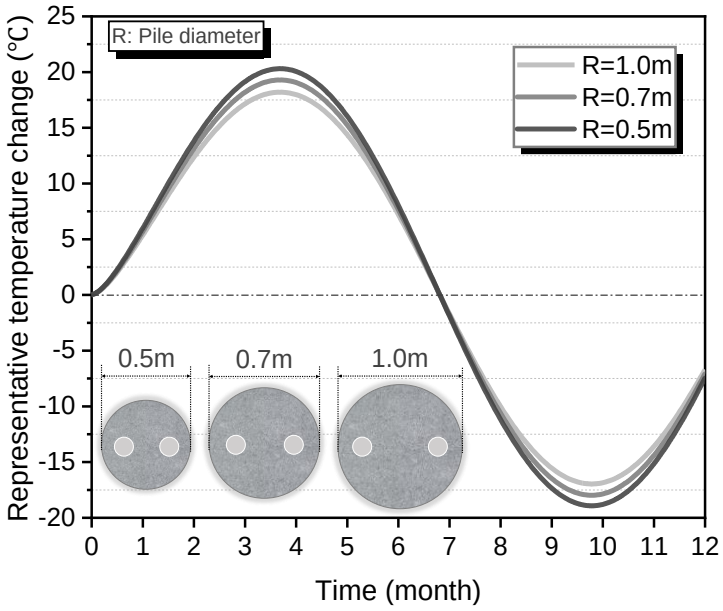

Fig.20 The representative temperature change for energy piles with a different pile diameter

5. Discussions and recommendations for energy pile design

In this study, we develop an analytical model to determine the representative temperature change, which is used in the thermo-mechanical design of energy piles. The verification of the analytical model is divided into two parts. On the one hand, it is verified through the finite element model that the analytical model can reasonably reflect the change law of representative temperature changes with thermal operation time. On the other hand, the analytical model is validated through numerical simulation that it can provide a more accurate thermodynamic response and provide a reference for the design of energy piles. Also, this paper has investigated the influence of critical parameters such as thermal load forms, the layout of heat exchange pipes, and pile diameter.

In the investigation of the layout of heat exchange pipes on the representative temperature change, we found that the calculated results increase with the number of heat exchange pipes. The result is quite different from the study of Abdelaziz et al.[29], who found that the representative temperature change of the energy pile is unaffected by the number and configuration of heat exchange pipes. Nevertheless, it is interesting that many studies have found the thermal operation is closely related to the installation

form of heat exchange pipe of energy piles. The geometrical configuration includes W-shaped, spiral-shaped, coaxial, multi-pipe, helical, single, double, and triple U-shaped heat exchange pipe[2,47–52]. Gao et al.[47] investigated and compared the thermal absorption of W-shaped and U-shaped heat exchange pipes with various legs. The results showed that the W-shaped heat exchange pipe was the most efficient among them. Furthermore, Wood et al. [49] compared the thermal behavior of U-shaped and coaxial heat exchange pipes. They found that the U-shaped heat exchange pipe possessed a higher thermal coefficient. All these studies suggest that the geometrical arrangements of heat exchange pipe have a strong influence on the thermal solicitations of energy piles and the variations in operating temperature. The analytical model proposed in this study can reflect the influence of heat exchange pipe configuration on the representative temperature change utilized for the thermomechanical design of energy piles.

The influence of heat exchange pipe installation form and pile diameter on the representative temperature is mainly reflected by the concrete thermal resistance in the analytical model[46,53–56]. According to the Eq. (10), the thermal resistance of different diameter piles and various heat exchange pipes is calculated and presented in Fig.21. It can be found that the thermal resistance decreases as the number of heat exchange pipes increase. However, it increases as the pile diameter increases. This reveals well why the representative temperature varies widely in the case of a large number of heat exchange pipes and small pile diameter.

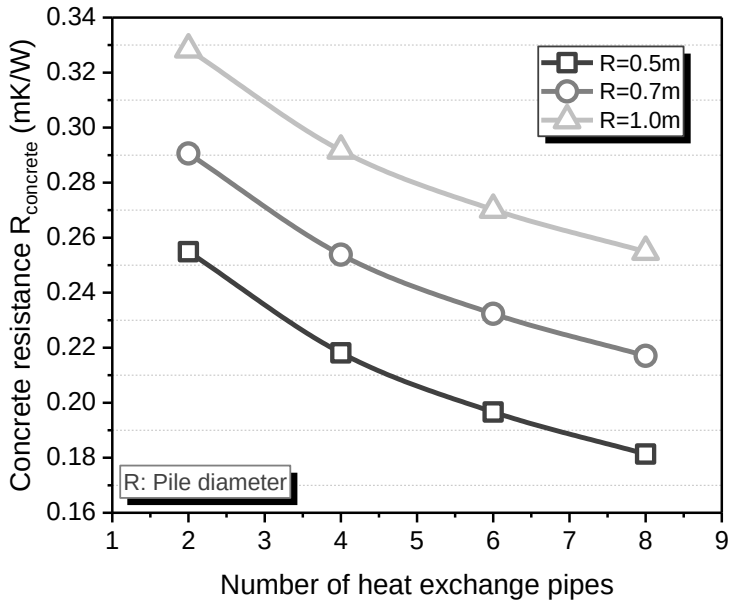

Fig.21 Thermal resistance comparison for different diameter piles and various heat exchange pipes.

To further theoretically explore the influence of thermal resistance, pile diameter, and the number of heat exchange pipes on the representative temperature change, we tried to establish a suitable theoretical formula based on the heat transfer analysis to explain what this study presented results. According to the schematic diagram of heat transfer analysis in a pile based on one-dimensional thermal resistance theory, shown in Fig.4, the temperature increment of the concrete can be written as

$$\Delta T(r) = \frac{qR_{concrete}}{r_{eq} - r_{pile}} r \tag{21}$$

According the Eq. (5), the increment of the average temperature change for the pile cross-section can be written as

$$\Delta T_{average}^{incre.} = \frac{r_{eq} + r_{pile}}{r_{eq} - r_{pile}} \frac{qR_{concrete}}{2} \tag{22}$$

Substituting for the thermal resistance of the concrete from Eq. (10), the Eq. (22) can be written as

$$\Delta T_{average}^{incre.} = \frac{r_{eq} + r_{pile}}{r_{eq} - r_{pile}} \frac{q \ln(r_{pile} / r_{eq})}{4\pi\lambda_{\text{concrete}}} \tag{23}$$

Define $\xi = \frac{r_{eq}}{r_{pile}}$, then $\xi \in (0,1)$. The thermal resistance of pile concrete and Eq. (23) can be respectively written as

$$R_{\text{concrete}} = \frac{-\ln(\xi)}{2\pi\lambda_{\text{concrete}}} \tag{24}$$

$$\Delta T_{average}^{incre.} = \frac{1+\xi}{1-\xi}\frac{q\ln(\xi)}{4\pi\lambda_{\text{concrete}}} \tag{25}$$

When $\xi \in (0,1)$, the Eq. (25) is increasing function. When $\xi \to 0$, i.e., $r_{eq} \to 0$, the thermal resistance of pile concrete increases and the increment of the average temperature change is small and closed to the temperature change of the pile wall; when $\xi \to 1$, i.e., $r_{eq} \to r_{pile}$, the thermal resistance of pile concrete decreases and the increment of the average temperature change is big and closed to the temperature change of the pipe wall. The increment of the average temperature change for the pile cross-section should be positively correlated based on the analysis of sections 2.2 and 2.3. According to the Eq. (25), the results of sections 4.3 and 4.4 will be discussed separately below.

For the case that effect of the layout of heat exchange pipes, the results mentioned in section 4.3 show that the representative temperature change is positively related to the number of heat exchange pipes while the pile diameter is constant. That is to say, for a given pile diameter, the more the number of heat exchange pipes, the larger the area of the equivalent pipe, the smaller the concrete area, and the smaller the corresponding thermal resistance. This situation means that the value of ξ gradually increases with the number of heat exchange pipes. According to Eq. (25), the calculated representative temperature change should increase, which is agree with the results obtained in section 4.3. For the case that effect of the pile diameter, the results obtained in section 4.4 present that the representative temperature change decreases with the pile diameter increasing. The increase in pile diameter makes the relative thermal resistance of the pile concrete more significant and means that the value of ξ decreases, according to Eq. (25), which indicates further that the calculated representative temperature change decreases. Thus, through the above analysis, it can be seen that there is a negative correlation between the thermal resistance of the pile concrete and

the representative temperature change, i.e., the smaller the thermal resistance, the greater the representative temperature change, and the greater the thermal resistance, the smaller the representative temperature.

Overall, the findings of this study suggest that whether the non-uniform temperature changes over the pile cross-section are taken into account will lead to a large difference in the thermomechanical design for energy piles. In experimental tests of energy piles, thermistors and strain gauges should be reasonably installed over the pile cross-section to reliably monitor the thermal temperature variations and deformations since the non-uniform temperature change occurs to the pile cross-section. It is worth noting that some limitations in this paper should be pointed out. The proposed model's applicability in a greater range of pile geometries should be assessed in the future. Additionally, it can be seen that the steady-state assumption of heat transfer in a pile will overestimate the representative temperature change[46]. Thus, the analytical model can be further developed to better account for the transient condition, which is especially important for larger diameter energy piles.

6. Conclusions

An analytical model has been proposed to calculate the representative temperature for the thermomechanical design of energy piles in this study. The overall goal of this paper is achieved in two steps: (i) Deriving the average temperature change through analyzing the relationship between the non-uniform temperature change and strains over the cross-section. (ii) Then proposing the concept and calculation method of the representative temperature change for energy pile design. This paper firstly has validated the correctness and robustness of the finite element method by comparing the thermomechanical responses obtained by the numerical simulations and that obtained by model tests and field tests. Then, the reliability and feasibility of the analytical model are verified by comparisons with the results of the finite element models, and the influence of critical parameters is investigated comprehensively. The main conclusions are summarized as follows.

(1) The expression of the average temperature change of the pile cross-section is derived according to the assumption of deforming uniformly for the pile section, and then the analytical model to calculate the representative temperature change is proposed by further introduced the heat source model and thermal resistance model inside the pile.

(2) The validity of the proposed analytical model is verified by comparing the results of the analytical model and the finite-element model. Besides, the comparison results show that the integral average temperature change used for the thermo-mechanical design of the energy pile for the pile depth is more representative than the average temperature change over the pile cross-sections.

(3) The results show that the analytical model can reflect the impact of the thermal load variations on the representative temperature change of energy pile by applying three different thermal load variations.

(4) The variations of relative thermal resistance make the representative temperature change with the pile diameter and heat exchange pipe configuration, and an increase in the number of heat exchange pipes or a decrease in pile diameter will increase the representative temperature change.

Acknowledgments

This research has been supported by the National Natural Science Foundation of China (Grants No. 51778107, 52078103), the China National Key R&D Program during the 13th Five-year Plan Period (Grant No. 2018YFC1505104 and 2017YFC1503103) and Liao Ning Revitalization Talents Program (Grants No. XLYC1807263).

Reference

1. Kong G, Wu D, Liu H, Laloui L, Cheng X, Zhu X. Performance of a geothermal energy deicing system for bridge deck using a pile heat exchanger. *Int J Energy Res*. 2019;43(1):596-603. doi:10.1002/er.4266
2. Sani AK, Singh RM, Amis T, Cavarretta I. A review on the performance of

geothermal energy pile foundation, its design process and applications. *Renew Sustain Energy Rev*. 2019;106(July 2018):54-78. doi:10.1016/j.rser.2019.02.008
3. Suryatriyastuti ME, Mroueh H, Burlon S. Understanding the temperature-induced mechanical behaviour of energy pile foundations. *Renew Sustain Energy Rev*. 2012;16(5):3344-3354. doi:10.1016/j.rser.2012.02.062
4. Batini N, Rotta Loria AF, Conti P, Testi D, Grassi W, Laloui L. Energy and geotechnical behaviour of energy piles for different design solutions. *Appl Therm Eng*. 2015;86:199-213. doi:10.1016/j.applthermaleng.2015.04.050
5. Olgun CG, Ozudogru TY, Abdelaziz SL, Senol A. Long-term performance of heat exchanger piles. *Acta Geotech*. 2015;10(5):553-569. doi:10.1007/s11440-014-0334-z
6. Murphy KD, McCartney JS. Seasonal Response of Energy Foundations During Building Operation. *Geotech Geol Eng*. 2015;33(2):343-356. doi:10.1007/s10706-014-9802-3
7. Bourne-webb PJ, Soga K, Amatya BL. A framework for understanding energy pile behaviour. *Geotech Eng*. 2013;166(GE2):170-177. doi:10.1680/geng.10.00098
8. Knellwolf C, Peron H, Laloui L. Geotechnical Analysis of Heat Exchanger Piles. *J Geotech Geoenvironmental Eng*. 2011;137(10):890-902. doi:10.1061/(ASCE)GT.1943-5606.0000513
9. Suryatriyastuti ME, Mroueh H, Burlon S. A load transfer approach for studying the cyclic behavior of thermo-active piles. *Comput Geotech*. 2014;55:378-391. doi:10.1016/j.compgeo.2013.09.021
10. Chen D, McCartney JS. Parameters for Load Transfer Analysis of Energy Piles in Uniform Nonplastic Soils. *Int J Geomech*. 2016;17(7):04016159. doi:10.1061/(asce)gm.1943-5622.0000873
11. Wood CJ, Liu H, Riffat SB. Comparison of a modelled and field tested piled ground heat exchanger system for a residential building and the simulated effect of assisted ground heat recharge. *Int J Low-Carbon Technol*. 2010;5(3):137-143.
12. Olgun CG, Ozudogru TY, Arson CF. Thermo-mechanical radial expansion of heat exchanger piles and possible effects on contact pressures at pile–soil interface. *Geotech Lett*. 2014;4(july-september):170-178. doi:10.1680/geolett.14.00018
13. Rotta Loria AF, Vadrot A, Laloui L. Effect of non-linear soil deformation on the interaction among energy piles. *Comput Geotech*. 2017;86:9-20. doi:10.1016/j.compgeo.2016.12.015
14. Park S, Lee S, Oh K, Kim D, Choi H. Engineering chart for thermal performance of cast-in-place energy pile considering thermal resistance. *Appl Therm Eng*. 2018;130:899-921. doi:10.1016/j.applthermaleng.2017.11.065
15. Yuanlong Cui JZ. Year-round performance assessment of a ground source heat pump with multiple energy piles. *Energy Build*. 2018;158:509-524.
16. Laloui L, Nuth M, Vulliet L. Experimental and numerical investigations of the

behaviour of a heat exchanger pile. *Int J Numer Anal Methods Geomech*. 2006;30(8):763-781. doi:10.1002/nag.499
17. Murphy KD, McCartney JS, Henry KS. Evaluation of thermo-mechanical and thermal behavior of full-scale energy foundations. *Acta Geotech*. 2015;10(2):179-195. doi:10.1007/s11440-013-0298-4
18. Sutman M, Brettmann T, Olgun CG. Full-scale in-situ tests on energy piles: Head and base-restraining effects on the structural behaviour of three energy piles. *Geomech Energy Environ*. 2019;18:56-68. doi:10.1016/j.gete.2018.08.002
19. Rammal D, Mroueh H, Burlon S. Impact of thermal solicitations on the design of energy piles. *Renew Sustain Energy Rev*. 2018;92(April):111-120. doi:10.1016/j.rser.2018.04.049
20. McCartney JS, Murphy KD. Investigation of potential dragdown/uplift effects on energy piles. *Geomech Energy Environ*. 2017;10:21-28. doi:10.1016/j.gete.2017.03.001
21. Laloui L, Dove JE, Filz GM. Thermo-Mechanical Behavior of Energy Piles: Full-Scale Field Testing and Numerical Modeling. Published online 2016.
22. Ghasemi-Fare O, Basu P. Influences of ground saturation and thermal boundary condition on energy harvesting using geothermal piles. *Energy Build*. 2018;165:340-351. doi:10.1016/j.enbuild.2018.01.030
23. Zarrella A, Emmi G, Zecchin R, De Carli M. An appropriate use of the thermal response test for the design of energy foundation piles with U-tube circuits. *Energy Build*. 2017;134:259-270. doi:10.1016/j.enbuild.2016.10.053
24. Ng CWW, Gunawan A, Shi C, Ma QJ, Liu HL. Centrifuge modelling of displacement and replacement energy piles constructed in saturated sand: A comparative study. *Geotech Lett*. 2016;6(1):34-38. doi:10.1680/jgele.15.00119
25. Xu D, Xu X, Li W, Fatahi B. Field experiments on laterally loaded piles for an offshore wind farm. *Mar Struct*. 2020;69:102684. doi:10.1016/j.marstruc.2019.102684
26. Meng K, Cui C, Li H. An Ontology Framework for Pile Integrity Evaluation Based on Analytical Methodology. *IEEE Access*. 2020;8:72158-72168. doi:10.1109/ACCESS.2020.2986229
27. Meng K, Cui C, Liang Z, Li H, Pei H. An Analytical Solution for Longitudinal Impedance of a Large-Diameter Floating Pile in Soil with Radial Heterogeneity and Viscous-Type Damping. *Appl Sci*. 2020;10(14):4906.
28. Abdelaziz S, Ozudogru TY. Non-uniform thermal strains and stresses in energy piles. *Environ Geotech*. 2016;3(4):237-252. doi:10.1680/jenge.15.00032
29. Abdelaziz SL, Ozudogru TY. Selection of the design temperature change for energy piles. *Appl Therm Eng*. 2016;107:1036-1045. doi:10.1016/j.applthermaleng.2016.07.067
30. Bourne-Webb PJ, Bodas Freitas TM. Thermally-activated piles and pile groups under monotonic and cyclic thermal loading–A review. *Renew Energy*. 2020;147:2572-2581. doi:10.1016/j.renene.2018.11.025
31. Rotta Loria AF. Performance-based Design of Energy Pile Foundations. *DFI*

Journal-The J Deep Found Inst. 2018;12(2):94-107.
32. Kakaç S, Yener Y, Naveira-Cotta CP. *Heat Conduction*. CRC Press; 2018.
33. Zeng HY, Diao NR, Fang ZH. A finite line-source model for boreholes in geothermal heat exchangers. *Heat Transf Res*. 2010;31(7):558–567.
34. Yavuzturk C. Modeling of vertical ground loop heat exchangers for ground source heat pump systems. Published online 1999.
35. Bernier MA. Ground-coupled heat pump system simulation/Discussion. *ASHRAE Trans*. 2001;107:605.
36. Gu Y, O'Neal DL. Development of an equivalent diameter expression for vertical U-tubes used in ground-coupled heat pumps. *ASHRAE Trans*. 1998;104(2):347-355.
37. Incropera FP, Lavine AS, Bergman TL, DeWitt DP. *Fundamentals of Heat and Mass Transfer*. Wiley; 2007.
38. Manual ASU. Abaqus 6.11. *http://130149*. 89(2080):v6.
39. Lazzari S, Priarone A, Zanchini E. Long-term performance of BHE (borehole heat exchanger) fields with negligible groundwater movement. *Energy*. 2010;35(12):4966-4974. doi:10.1016/j.energy.2010.08.028
40. Dupray F, Bachler M, Laloui L. *Effect of Groundwater Flow on the THM Behavior of an Energy Pile*. CRC Press, Boca Raton, FL, USA; 2013.
41. Manassero M, Dominijanni A, Foti S, Musso G. *Coupled Phenomena in Environmental Geotechnics*. CRC Press; 2013.
42. Ng CWW, Ma QJ, Gunawan A. Horizontal stress change of energy piles subjected to thermal cycles in sand. *Comput Geotech*. 2016;78:54-61. doi:10.1016/j.compgeo.2016.05.003
43. Lee CJ, Ng CWW. Development of Downdrag on Piles and Pile Groups in Consolidating Soil. *J Geotech Geoenvironmental Eng*. 2004;130(9):905-914. doi:10.1061/(ASCE)1090-0241(2004)130:9(905)
44. Song H, Pei H, Xu D, Cui C. Performance study of energy piles in different climatic conditions by using multi-sensor technologies. *Measurement*. Published online 2020:107875. doi:https://doi.org/10.1016/j.measurement.2020.107875
45. Cullin JR, Spitler JD. A computationally efficient hybrid time step methodology for simulation of ground heat exchangers. *Geothermics*. 2011;40(2):144-156. doi:10.1016/j.geothermics.2011.01.001
46. Loveridge FA, Powrie W. The Average Temperature of Energy Piles. In: *Geo-Chicago 2016*. ; 2016:166-175.
47. Gao J, Zhang X, Liu J, Li K, Yang J. Numerical and experimental assessment of thermal performance of vertical energy piles: An application. *Appl Energy*. 2008;85(10):901-910. doi:10.1016/j.apenergy.2008.02.010
48. Park H, Lee SR, Yoon S, Choi JC. Evaluation of thermal response and performance of PHC energy pile: Field experiments and numerical simulation. *Appl Energy*. 2013;103:12-24. doi:10.1016/j.apenergy.2012.10.012
49. Wood CJ, Liu H, Riffat SB. Comparative performance of 'U-tube'and 'coaxial'loop designs for use with a ground source heat pump. *Appl Therm*

Eng. 2012;37:190-195.
50. Miyara A, Tsubaki K, Inoue S, Yoshida K. Experimental study of several types of ground heat exchanger using a steel pile foundation. *Renew Energy*. 2011;36(2):764-771.
51. Yoon S, Lee S-R, Xue J, Zosseder K, Go G-H, Park H. Evaluation of the thermal efficiency and a cost analysis of different types of ground heat exchangers in energy piles. *Energy Convers Manag*. 2015;105:393-402.
52. Zarrella A, De Carli M, Galgaro A. Thermal performance of two types of energy foundation pile: Helical pipe and triple U-tube. *Appl Therm Eng*. 2013;61(2):301-310. doi:10.1016/j.applthermaleng.2013.08.011
53. Javed S, Spitler JD. Accuracy of borehole thermal resistance calculation methods for grouted single U-tube ground heat exchangers. *Appl Energy*. 2017;187:790-806. doi:10.1016/j.apenergy.2016.11.079
54. Loveridge F, Powrie W. 2D thermal resistance of pile heat exchangers. *Geothermics*. 2014;50:122-135. doi:10.1016/j.geothermics.2013.09.015
55. Sani AK, Singh RM, Tsuha C de HC, Cavarretta I. Pipe–pipe thermal interaction in a geothermal energy pile. *Geothermics*. 2019;81(December 2018):209-223. doi:10.1016/j.geothermics.2019.05.004
56. Loveridge F. The Thermal Performance of Foundation Piles used as Heat Exchangers in Ground Energy Systems. *Univ Southhampt*. Published online 2012:206. http://eprints.soton.ac.uk/348910/1.hasCoversheetVersion/F Loveridge eThesis FINAL.pdf